Solar Energy Materials & Solar Cells 136 (2015) 86–91

Contents lists available at ScienceDirect

Solar Energy Materials & Solar Cells

journal homepage: www.elsevier.com/locate/solmat

High-performance ITO-free electrochromic films based on bi-functional stacked WO_3/Ag/WO_3 structures

Hailing Li [a,b], Ying Lv [a], Xin Zhang [c], Xiaoyi Wang [c], Xingyuan Liu [a,*]

[a] State Key Laboratory of Luminescence and Applications, Changchun Institute of Optics, Fine Mechanics and Physics, Chinese Academy of Sciences, Changchun 130033, China
[b] University of Chinese Academy of Sciences, Beijing 100049, China
[c] Key Laboratory of Optical System Advanced Manufacturing Technology, Chinese Academy of Sciences, Changchun 130033, China

ARTICLE INFO

Article history:
Received 26 August 2014
Received in revised form
31 December 2014
Accepted 2 January 2015
Available online 22 January 2015

Keywords:
Electrochromism
WO_3/Ag/WO_3
Transparent conductor
Dielectric-metal-dielectric

ABSTRACT

Stacked WO_3/Ag/WO_3 (WAW) films were employed as both transparent electrodes and electrochromic materials. These nontoxic, low-cost WAW films that were prepared at room temperature exhibited not only low sheet resistance (12.2 Ω/□) and high transmittance (> 80%) but also compelling electrochromic performance with high optical contrast (53%) at 650 nm, long-term cycling stability (3000 cycles), and short switching time (coloration time = 11 s; bleaching time = 10.5 s). The coloration efficiency of the WAW films was 136 cm^2 C^{-1}, which is higher than those of most electrochromic transition metal oxides. In addition, by utilizing such bi-functional films, the flexible electrochromic film with acceptable performance was obtained.

1. Introduction

Electrochromism is the phenomenon of certain materials reversibly changing their colors through redox reactions under the influence of an external electric field [1]. It has found applications in many fields including smart windows, mirrors, and electrochromic displays [2]. A traditional electrochromic device (ECD) has the following layered structure: substrate / transparent conductor (TC) / electrochromic (EC) film / electrolyte (IC) / ion reservoir / electrode / substrate [3,4]. Generally, the TC is required to be transparent and should possess a minimum resistance. Indium tin oxide (ITO), one of the most commonly used materials for transparent electrode films [5,6], is expensive owing to the rarity and fast depletion of the element indium. In addition, it is so brittle that it can not withstand repetitive bending. These attributes render ITO disadvantageous for low-cost flexible devices [7]. Also, given the increased focus on energy savings and environmental protection, the development of low-cost transparent electrodes is now a prerequisite for energy-efficient ECDs.

Recently, dielectric–metal–dielectric (DMD) structures have aroused great interest as transparent conductive electrodes with good optical and electrical properties [8–10]. Metals such as Ag, Au, and Cu and various low-cost dielectric materials such as SnO_2, ZnS, and TiO_2 have been evaluated as candidate materials for the DMD structure. It has been shown that the transmittance and conductivity of a DMD electrode can be optimized by tuning the thickness of the dielectric and metal layers.

One of the frequently used dielectric materials for DMD structures, WO_3, is also a widely studied electrochromic material [11]. Therefore, it is feasible to employ WO_3 as a low-cost material in DMD electrodes that integrates the functions of both a TC and an EC material. Recently, such an idea was realized through an electrochromic device based on a WO_3/Ag/WO_3 (WAW) transparent conductor [12]. However, to protect the middle Ag layer, a very thick outer WO_3 layer (> 300 nm) was used, which led to a low optical contrast in the visible-light region, accompanied by low electrochromic stability. Moreover, the general advantages of DMD electrodes were not observed.

In this article, we will demonstrate that high transmittance and conductance can be achieved for low-cost WAW films with a very thin outer WO_3 layer (< 70 nm) on both rigid and flexible substrates at room temperature. These WAW films were found to act simultaneously as an electrode and an electrochromic layer, thereby allowing for the simplification of ECD construction. Wide optical modulation, short response time, high cycling stability, and high coloration efficiency have been obtained in rigid electrochromic films. As a state-of-art application, a bi-functional WAW film was used to construct a flexible electrochromic film, which exhibited an acceptable performance.

2. Experimental

The glass and polyethylene terephthalate (PET) substrates were ultrasonically cleaned with acetone, ethanol, and deionized water successively, and finally dried in an oven. The WAW films were

* Corresponding author. Tel.: +86 0431 86176341.
E-mail address: liuxy@ciomp.ac.cn (X. Liu).

http://dx.doi.org/10.1016/j.solmat.2015.01.002
0927-0248/

thermally deposited sequentially at room temperature on the cleaned glass or PET substrates by electron-beam evaporation. Prior to deposition, the background pressure was set to below 3.8×10^{-3} Pa. The evaporation rates of WO_3 and Ag were 0.3 and > 0.8 nm s^{-1}, respectively. The optical characteristics of the films were evaluated with a spectrophotometer (UV-3101PC, Shimadzu, Japan). The surface resistances of the films were measured by a four-point probe instrument equipped with a surface-resistivity meter. The bending properties of flexible WAW electrodes were investigated using a lab-made cyclic bending test system with a bending radius of 15 mm and a bending angle of 90°. The cyclic bending tests were carried out at a frequency of 1.0 Hz over duration of 1600 cycles. The optical constants of WO_3 and Ag films for the simulations were measured by an Ellipsometer (UVISEL, HORIBA Jobin Yvon, France). The film morphologies were examined with atomic force microscopy (AFM; SA400HV, Seiko Instruments, Japan).

All the electrochemical measurements were recorded on a CHI 920 electrochemical workstation (Shanghai Chenhua Instruments Inc., China). The electrochromic properties of the films were measured using a standard three-electrode system, with WAW or ITO/WO_3 as the working electrode, a titanium plate as the counter electrode, and Ag/AgCl (3.5 M KCl) as the reference electrode. The electrolyte used was 1 M lithium perchlorate–propylene carbonate (both $LiClO_4$ and PC were purchased from Aladdin, China), which was bubbled with nitrogen for 30 min before the electrochemical measurements were recorded. Cyclic voltammetry (CV) and chronoamperometry (CA) were carried out to study long-term stability and response time, respectively. The equipment used for CA was fitted with a custom-made optical transmittance spectroscope equipped with a reflector lamp as the light source and a Maya 2000 spectrometer (spectral range: 380–820 nm).

For rigid ECDs, the patterned WAW films acted as the working electrode (1.8 cm × 1.8 cm), while another unpatterned WAW or ITO film (1.8 cm × 1.8 cm) served as the counter electrode. The ECDs were sealed with patterned, 120-μm-thick heat-sealable films, which also worked as spacers between the two electrodes. Finally, the cavities formed between the two electrodes were injected with 1 M $LiClO_4$–PC electrolyte and then sealed using a UV-curing adhesive at the end. All measurements were performed in air at room temperature.

3. Results and discussion

The transmittance spectra of the WAW films were simulated based on the optical-transfer matrix method [13,14]. The characteristic matrix of a WAW film on a glass substrate is as follows:

$$\begin{bmatrix} B \\ C \end{bmatrix} = \left\{ \prod_{j=1}^{3} \begin{bmatrix} \cos\delta_j & \frac{i}{\eta_j}\sin\delta_j \\ i\eta_j \sin\delta_j & \cos\delta_j \end{bmatrix} \right\} \begin{bmatrix} 1 \\ \eta_4 \end{bmatrix} \quad (1)$$

$$\eta_j = \begin{cases} N_j/\cos\theta_j & \text{for } p-\text{polarized wave} \\ N_j \cos\theta_j & \text{for } s-\text{polarized wave} \end{cases} \quad (2)$$

where j=0 (for the incidence medium); 1, 2, or 3 for the WAW layers; or 4 for the substrate. The angular phase thickness is

$$\delta_j = \frac{2\pi}{\lambda} N_j d_j \cos\theta_j \quad (3)$$

where θ_j is the angle of wave propagation in the layer as determined from Snell's law, and N_j denotes the complex refractive index of each layer for the incident wavelength λ. The thicknesses of the WO_3 layer exposed to air, the Ag layer, and the WO_3 layer on the glass substrate are represented by d_3, d_2, and d_1, respectively (hereafter abbreviated as $d_1/d_2/d_3$). Their transmittance can be calculated as

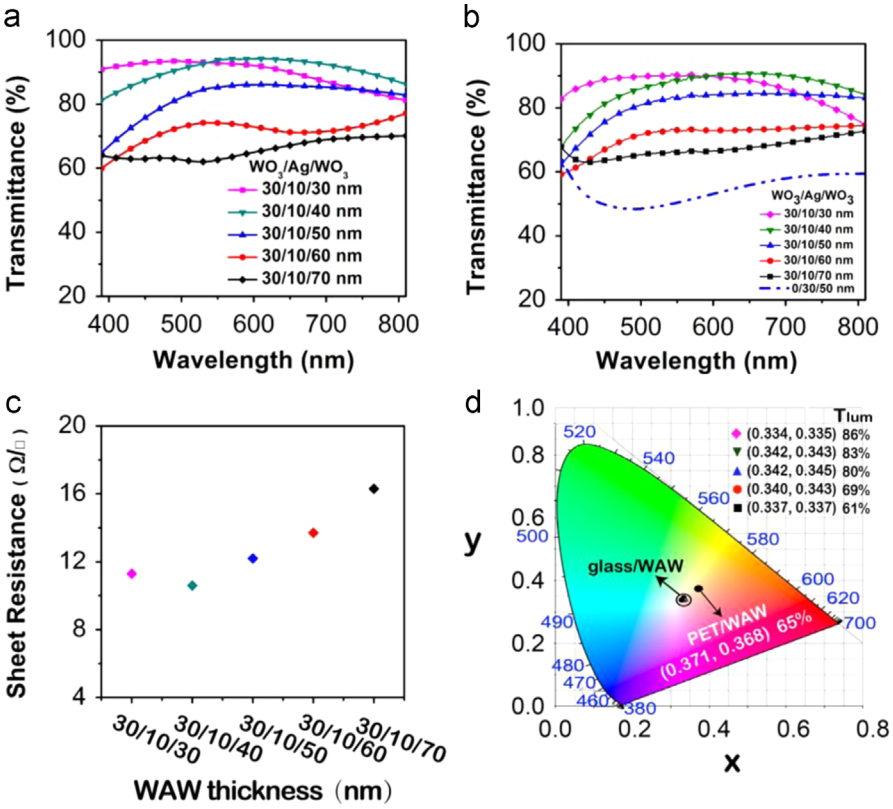

Fig. 1. (a) Calculated transmittance spectra, (b) measured transmittance spectra, and (c) sheet resistances of glass/WAW films with varying thickness (30–70 nm) of the outer WO_3 layers. (d) Chromaticity coordinates and luminous transmittance (T_{lum}) of glass/WAW and PET/WAW films.

$$T = \frac{4\eta_0\eta_4}{(\eta_0 B + C)^2} \quad (4)$$

The simulated results are shown in Fig. 1a. It was observed that the transmittance of the WAW films could be easily modulated by simply changing the thickness of the outer WO_3 layer. As the outer WO_3 layer thickness increased, the mean transmittance in visible light gradually decreased. Fig. 1b shows the measured transmittance spectra of the WAW films, which are reasonably consistent with the simulated results. All WAW films showed high average transmittance (> 60%) in the visible region, together with a significantly low sheet resistance of $13 \pm 3\ \Omega/\square$ (Fig. 1c), both of which could help improve the optical contrast and response speed of electrochromic films. In order to study the effect of the bottom WO_3 layer on the transmittance of electrodes, we compared the average transmittance (400–700 nm) of WAW (30/10/50 nm) and Ag/WO_3 (10/50 nm, hereafter referred to as AW). The mean transmittance of AW film in visible light is only 52.7%, which is significantly lower than that of WAW film (80.9%). Therefore, the bottom WO_3 layer is critical for achieving high transmittance of the electrodes.

The Commission of International de L'Eclairage (CIE, 1931) chromaticity coordinates and the integrated luminous transmittance (T_{lum}) (400–700 nm) for all glass/WAW films (transparent state) are illustrated in Fig. 1d. T_{lum} is obtained from,

$$T_{lum} = \int \varphi_{lum}(\lambda) T_{(\lambda)} d\lambda / \varphi_{lum}(\lambda) d\lambda \quad (5)$$

where $T(\lambda)$ represents the spectral transmittance, φ_{lum} is the sensitivity of the light-adapted human eye [15,16]. All WAW films have the similar color coordinates near white light area and display high T_{lum} (> 60%), which indicates that they are almost colorless, and meet the requirements of practical architectural windows [17]. Based on the above results, we chose WAW films with thicknesses of 30 nm for the bottom WO_3 layer, 10 nm for the Ag layer, 40 and 50 nm for the top WO_3 layers to study their electrochromic properties due to their excellent transmittance (> 80%) in the visible region and high conductivity (< 13 $\Omega/\square$).

The electrochromic characteristics, such as contrast ratio (ΔT), response time, and coloration efficiency (η) of the WAW films were systematically evaluated. A single WO_3 film (50 nm) on an ITO (20 $\Omega/\square$) electrode (hereafter referred to as ITO/WO_3) was also studied for comparison. In general, when WO_3 films are cathodically polarized, they display a uniform blue color that intensifies with increasing cathodic potential [18,19]. On the other hand, when these blue WO_3 films are anodically polarized, they are bleached and become transparent. Fig. 2a shows the transmittance of WAW (30/10/50 nm) films on glass at various potentials. The WAW film exhibited advanced light modulation in the visible-light range, accompanied by a high average optical contrast ($\Delta T = T_b - T_c$, where T_b represents the transmittance in the bleached state and T_c represents the transmittance in the colored state) of 45% and a maximum ΔT of 53% at 650 nm when the potential was changed in steps between 0.6 and –0.6 V vs. Ag/AgCl. In comparison, ΔT at 650 nm for the ITO/WO_3 film under the same condition was only 24% (Fig. 2b). We had to increase the negative potential in order to enhance the optical contrast. The maximum ΔT at 650 nm for WAW' (30/10/40 nm) is 46%, which is slightly lower than that of WAW (30/10/50 nm). Therefore, WAW with 50 nm top WO_3 layer was chosen for further study.

The response time (τ) is a key parameter for evaluating the electrochromic performance, and it is defined as the time taken by the transmittance to reach a value of 90% of total transmittance variation [20]. As can be seen in Fig. 2b, the coloration time (τ_c) and bleaching time (τ_b) of the WAW electrochromic film were 11 s and 10.5 s, respectively. The average response time of the WAW

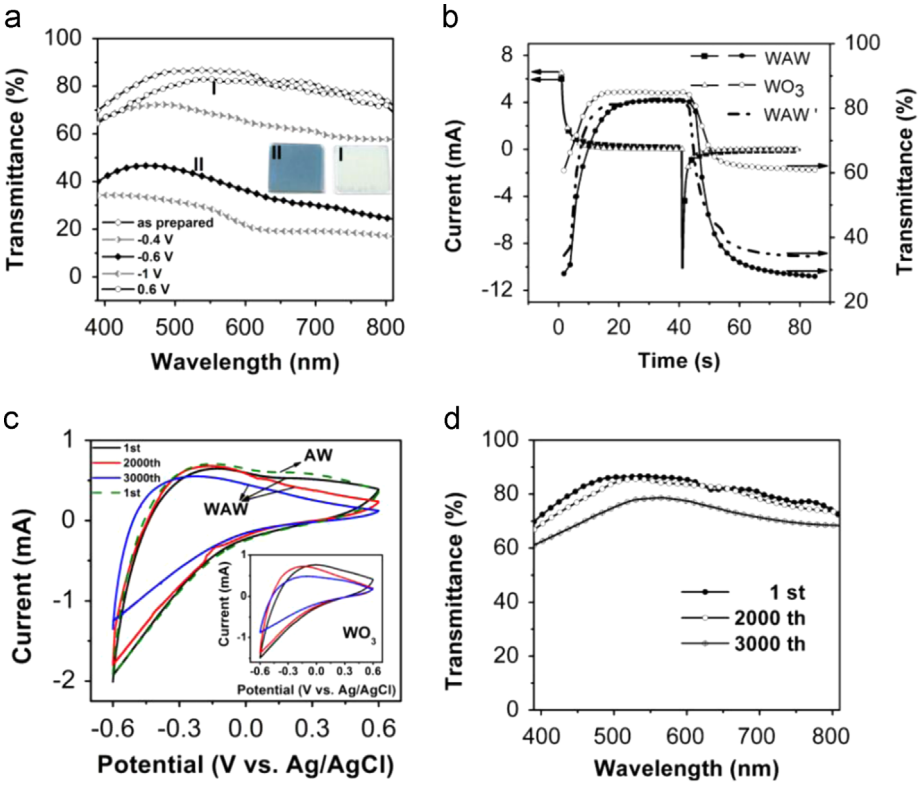

Fig. 2. (a) Variations in transmittance with different voltages; the inset shows photographs of WAW films in bleached (I) (0.6 V) and colored (II) (–0.6 V) states. (b) Evolution of current and optical contrast of WAW (30/10/50 nm), WAW' (30/10/40 nm), and WO_3 (50 nm) films at 650 nm upon application of potential stepping from –0.6 to 0.6 V vs. Ag/AgCl with a 40 s interval. (c) CV curves of WAW, WO_3, and AW films at different scan cycles with a scan rate of 0.1 V s^{-1}. (d) Corresponding changes in transmittance of the WAW film after different scan cycles.

film was 1.75 s shorter than that of the ITO/WO_3 film. A response speed of several seconds is suitable for smart windows [21].

The coloration efficiency represents the change in optical density (ΔOD) at a given wavelength for the charge consumed per unit of electrode area [22]; it can be calculated using the following formulae:

$$\eta = (\Delta OD)/Q \tag{6}$$

$$\Delta OD = \log(T_b/T_c) \tag{7}$$

Here, Q is the injected electronic charge per unit area, and ΔOD is the change in optical density at a certain wavelength. The calculated η for the WAW film at 650 nm was 136 $cm^2\ C^{-1}$, which is two times larger than that of the ITO/WO_3 film (45 $cm^2\ C^{-1}$) and higher than the values for most electrochromic transition metal oxides [23–25].

In order to evaluate the overall electrochemical performances of the electrochromic films, here we propose a quality factor $\Gamma_{(\lambda)}$ as follows:

$$\Gamma_{(\lambda)} = \eta_{(\lambda)}/\tau, \tau = (\tau_c + \tau_b)/2 \tag{8}$$

Where $\eta_{(\lambda)}$ is the coloration efficiency at a given wavelength, τ is the mean value of the coloring and bleaching time. It stands to reason that a greater Γ leads to better electrochromic performance. Table 1 summarizes the overall electrochromic performances of the WAW and ITO/WO_3 films. The values of $\Gamma_{(650\ nm)}$ for a WAW film and a single WO_3 film were 12.65 and 3.6 $cm^2\ C^{-1}\ s^{-1}$, respectively, indicating that the electrochromic performance of the WAW film on glass was better than that of the ITO/WO_3 film on glass.

Table 1
Comparison of electrochromic properties[a] of glass/WAW and ITO/WO_3 films.

Material system	ΔT (%)	η ($cm^2\ C^{-1}$)	$(\tau_c+\tau_b)/2$ (s)	$\Gamma_{(650\ nm)}$ ($cm^2\ C^{-1}\ s^{-1}$)
WO_3/Ag/WO_3	53	136	10.75	12.65
WO_3	24	45	12.5	3.6

[a] The WO_3/Ag/WO_3 and WO_3 film properties were measured at 650 nm with potential stepping from –0.6 to 0.6 V vs. Ag/AgCl.

The cycling stability of the WAW film was examined by successive cyclic voltammetry (CV) scans. The CV curves were recorded for the first, 2000th and 3000th cycles at room temperature, measured in a 1 M $LiClO_4$–PC solution at a sweeping rate of 0.1 V s^{-1} between –0.6 and 0.6 V. As shown in Fig. 2c, the current response was nearly identical during the initial 2000 cycles, without any significant change in the shape of the CVs. After 3000 cycles, a slight decrease in the current and transmittance (Fig. 2d) was observed. Moreover, the sheet resistance of the WAW film increased from 12.2 to 28.7 Ω/□, implying the degradation of the Ag layer to some extent. The durability of the ITO/WO_3 film was also studied under the same conditions. The graph in the inset of Fig. 2c shows obvious degradation of WO_3 after 3000 cycles, which is speculated to be mainly caused by a slow degeneration of the WO_3 film in the electrolyte solution [26]. Furthermore, from the nearly identical CV curves of WAW and AW films, it can be suggested that the bottom WO_3 layer make large contribution to the transparency of electrodes, but negligible contribution to electrochromism.

These bi-functional WAW (30/10/50 nm) films were deposited on PET substrates (hereafter referred to as PET/WAW) to construct flexible devices. Fig. 3a shows the electrical characteristic of PET/WAW electrode with the sheet resistance increasing slightly from 23 Ω/□ to 23.9 Ω/□ after 1600 bending cycles. This illustrates that the PET/WAW electrode possessed a fairly stable mechanical property. Fig. 3b displays the chronoamperometry and optical contrast of the flexible WAW film at 650 nm upon application of potential stepping from –0.6 to 0.6 V vs. Ag/AgCl with a 40 s interval. The patterned flexible ECDs were also realized, as shown in Figs. 3c and 3d. As seen in Figs. 3c and 1d, the PET/WAW film is slightly yellowish with the chromaticity coordinates of (0.361, 0.359), and displays an acceptable T_{lum} of 65%. From Fig. 3b, we can see that the flexible WAW film exhibited an acceptable performance with an optical contrast of 25%, coloration efficiency of 138 $cm^2\ C^{-1}$, and response time of less than 30 s (τ_b=20 s; τ_c=26 s). Compared with the WAW film on glass, the WAW film

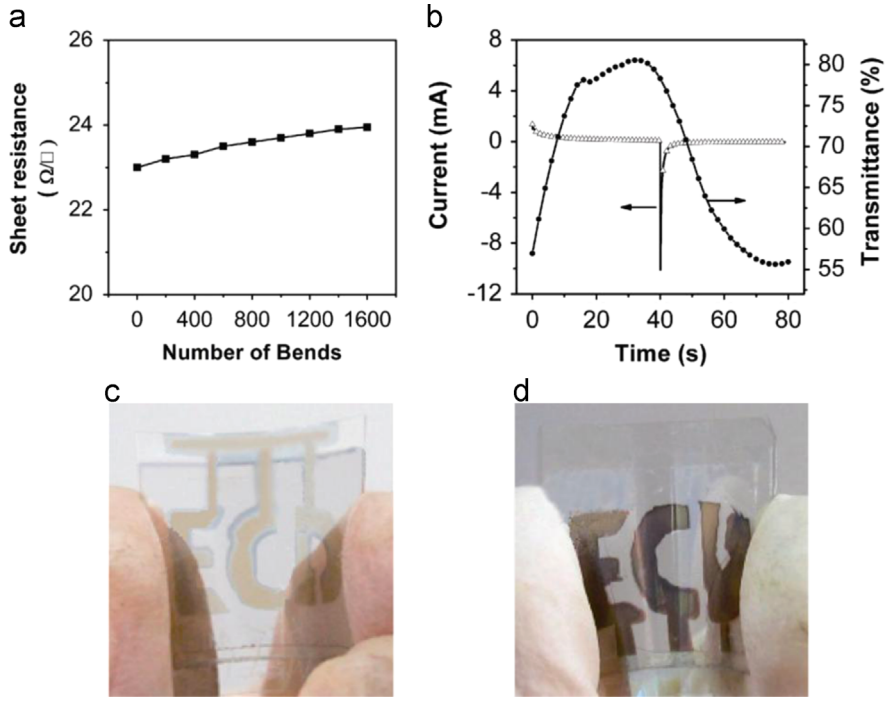

Fig. 3. (a) and (b) sheet resistance after repeated bending and electric-photo response of PET/WAW flexible electrode, correspondingly. (c) and (d) bleached and colored pictures of the WAW film on a PET substrate, respectively. Its measurement conditions were the same as those for the WAW film deposited on glass.

on PET displayed a relatively low quality factor $\Gamma_{(650\ nm)}$ (12.65 vs. 6 $cm^2\ C^{-1}\ s^{-1}$).

To study the reason for the lower performance of the flexible WAW film, we examined the surface morphology and conductivity of WAW films on glass and PET substrates. As shown in Fig. 4, we observed very smooth surfaces on a single glass and a glass/WAW film with root-mean-square (RMS) roughness of only 0.9 and 1.3 nm, respectively. In contrast, a single PET and a PET/WAW film presented some surface bumps, leading to a higher RMS roughness of 5.9 and 10.7 nm, respectively. The rough surface morphology of a single PET substrate would obviously reduce the continuity of 10 nm Ag layer, which results in the increase of PET/WAW film surface resistivity [27,28]. In fact, the sheet resistivity of the PET/WAW film is 23 Ω/□, which is nearly double that of the glass/WAW film (12.2 Ω/□). It has been established that the electrode resistance has a marked effect on the response time and optical contrast of an electrochromic film [29], and that a high electrode resistance leads to a non-uniform potential across the electrode (Ohmic loss) as well as a non-uniform current distribution in the electrolyte [30]. We believe that by further optimizing the thickness of each layer and using more uniform substrates, the performance of the flexible WAWs can be further improved.

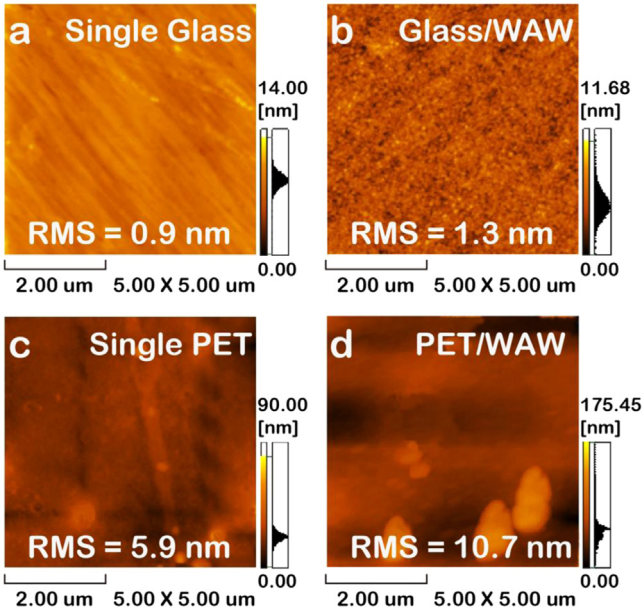

Fig. 4. AFM images of (a) single glass, (b) glass/WAW, (c) single PET, and (d) PET/WAW.

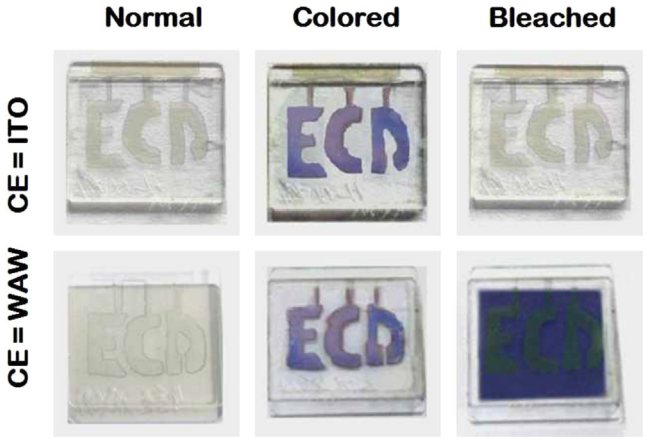

Fig. 5. ECDs with the WAW film as the working electrode and a single ITO (top photos) or WAW film (bottom photos) as the counter electrode.

Finally, as shown in Fig. 5, two kinds of electrochromic devices were obtained with a patterned WAW (30/10/50 nm) film as the working electrode, and a full-covered ITO or WAW film as the CE. Compared to the ECD (top line) based on the ITO CE, the text hidden or exposed in the patterned WAW film (second line) could be controlled reversibly by adjusting the potential applied on the working electrode, which indicates that it can be a promising candidate for applications in anti-counterfeiting and security authentication [31,32].

4. Conclusions

In summary, by utilizing low-cost, transparent conductive WAW films that serve simultaneously as an electrode and an electrochromic material, we realized non-toxic, high-performance, room-temperature-made, ITO-free electrochromic films that displayed high optical contrast (53% at 650 nm), long-term cycling stability (3000 cycles), and short switching time (τ_c=11 s; τ_b=10.5 s) at a low switching voltage of −0.6 to 0.6 V versus Ag/AgCl, which represent remarkable performance compared to that of single WO_3 film. In particular, the comprehensive parameter $\Gamma_{(650\ nm)}$ of the WAW film was even better than that of the ITO/WO_3 film (12.65 vs. 3.6 $cm^2\ C^{-1}\ s^{-1}$).

Moreover, this approach of utilizing bi-functional DMD electrodes to simplify the construction of ECDs was also extended to the fabrication of flexible devices, and an acceptably high level of performance was obtained. Our findings in this study could be applied to a novel strategy for constructing low-cost, high-performance ECDs, while employing similar composite structures of other transition-metal oxides liking V_2O_5 and MoO_3, and a few organic electrochromic materials such as polyaniline, polythiophene, and PEDOT.

Acknowledgments

This work is supported by the CAS Innovation Program, and National Science Foundation of China No. 51102228, and project supported by State Key Laboratory of Luminescence and Applications.

References

[1] F.C. Krebs, Electrochromic displays-the new black, Nat. Mater. 7 (2008) 766–767.
[2] P.M. Beaujuge, J.R. Reynolds, Color control in π-conjugated organic polymers for use in electrochromic devices, Chem. Rev. 110 (2010) 268–320.
[3] R.J. Mortimer, Electrochromic materials, Chem. Soc. Rev. 26 (1997) 147–156.
[4] V.K. Thakur, G. Ding, J. Ma, P.S. Lee, X. Lu, Hybrid materials and polymer electrolytes for electrochromic device applications, Adv. Mater. 24 (2012) 4071–4096.
[5] C. Xiang, W. Koo, F. So, H. Sasabe, J. Kido, A systematic study on efficiency enhancements in phosphorescent green, red and blue microcavity organic light emitting devices, Light: Sci. Appl. 2 (2013) e74.
[6] F. Pincella, K. Isozaki, K. Miki, A visible light-driven plasmonic photocatalyst, Light: Sci. Appl. 3 (2014) e133.
[7] S. De, T.M. Higgins, P.E. Lyons, E.M. Doherty, P.N. Nirmalraj, W.J. Blau, J.J. Boland, J.N. Coleman, Silver nanowire networks as flexible, transparent, conducting films: extremely high DC to optical conductivity ratios, ACS Nano 3 (2009) 1767–1774.
[8] M.C. Zhang, T.W. Allen, R.G. DeCorby, Experimental study of optimized surface-plasmon-mediated tunneling in metal-dielectric multilayers, Appl. Phys. Lett. 103 (2013) 071109.
[9] M.C. Gather, K. Meerholz, N. Danz, K. Leosson, Net optical gain in a plasmonic waveguide embedded in a fluorescent polymer, Nat. Photonics 4 (2010) 457–461.
[10] S. Schubert, J. Meiss, L. Müller-Meskamp, K. Leo, Improvement of transparent metal top electrodes for organic solar cells by introducing a high surface energy seed layer, Adv. Energy Mater 3 (2013) 438–443.

[11] B. Yang, Y. Zhang, E. Drabarek, P.R.F. Barnes, V. Luca, Enhanced photoelectrochemical activity of Sol-Gel tungsten trioxide films through textural control, Chem. Mater. 19 (2007) 5664–5672.
[12] G. Leftheriotis, E. Koubli, P. Yianoulis, Combined electrochromic-transparent conducting coatings consisting of noble metal, dielectric and WO3 multilayers, Sol. Energy Mater. Sol. Cells 116 (2013) 110–119.
[13] D.R. Lide, CRC Handbook of Chemistry and Physics, Boca Raton, Florida (2008).
[14] X. Liu, The design of ZnS/Ag/ZnS transparent conductive multilayer films, Thin Solid Films 441 (2003) 200–206.
[15] I. Bayrak Pehlivan, E.L. Runnerstrom, S.Y. Li, et al., A polymer electrolyte with high luminous transmittance and low solar throughput: Polyethyleneimine-lithium bis(trifluoromethylsulfonyl) imide with In2O3:Sn nanocrystals, Appl. Phys. Lett. 100 (2012) 241902.
[16] Y. Zhou, Y. Cai, X. Hu, et al., Temperature-responsive hydrogel with ultra-large solar modulation and high luminous transmission for "smart window" applications, J. Mater. Chem. A 2 (2014) 13550.
[17] C. Liu, X. Cao, A. Kamyshny, et al., VO(2)/Si-Al gel nanocomposite thermochromic smart foils: largely enhanced luminous transmittance and solar modulation, J. Colloid Interface Sci. 427 (2014) 49–53.
[18] J. Wang, E. Khoo, P.S. Lee, J. Ma, Synthesis, assembly, and electrochromic properties of uniform crystalline WO_3 nanorods, J. Phys. Chem. C 112 (2008) 14306–14312.
[19] C. Costa, C. Pinheiro, I. Henriques, C.A. Laia, Inkjet printing of sol-gel synthesized hydrated tungsten oxide nanoparticles for flexible electrochromic devices, ACS Appl. Mater. Interfaces 4 (2012) 1330–1340.
[20] F. Lin, J. Cheng, C. Engtrakul, A.C. Dillon, D. Nordlund, R.G. Moore, T.-C. Weng, S.K.R. Williams, R.M. Richards, In situ crystallization of high performing WO3-based electrochromic materials and the importance for durability and switching kinetics, J. Mater. Chem. 22 (2012) 16817–16823.
[21] R. Baetens, B.P. Jelle, A. Gustavsen, Properties, requirements and possibilities of smart windows for dynamic daylight and solar energy control in buildings: A state-of-the-art review, Sol. Energy Mater. Sol. Cells 94 (2010) 87–105.
[22] R.M.e. Osuna, V. Hernandez, J.T.L.o. Navarrete, E.I. Kauppinen, V. Ruiz, Ultrafast and high-contrast electrochromism on bendable transparent carbon nanotube electrodes, J. Phys. Chem. Lett. 1 (2010) 1367–1371.
[23] K. Lee, D. Kim, S. Berger, R. Kirchgeorg, P. Schmuki, Anodically formed transparent mesoporous TiO2 electrodes for high electrochromic contrast, J. Mater. Chem. 22 (2012) 9821–9825.
[24] F. Lin, D. Nordlund, T.C. Weng, D. Sokaras, K.M. Jones, R.B. Reed, D.T. Gillaspie, D.G. Weir, R.G. Moore, A.C. Dillon, R.M. Richards, C. Engtrakul, Origin of electrochromism in high-performing nanocomposite nickel oxide, ACS Appl. Mater. Interfaces 5 (2013) 3643–3649.
[25] Y.L. Xie, F.C. Cheong, Y.W. Zhu, B. Varghese, R. Tamang, A.A. Bettiol, C.H. Sow, Rainbow-like MoO3 Nanobelts, Fashioned via AFM Micromachining, J. Phys. Chem. 114 (2010) 120–124.
[26] D. Ma, G. Shi, H. Wang, Q. Zhang, Y. Li, Morphology-tailored synthesis of vertically aligned 1D WO_3 nano-structure films for highly enhanced electrochromic performance, J. Mater. Chem. A 1 (2013) 684–691.
[27] L. VJ, N.P. Kobayashi, M.S. Islam, et al., Ultrasmooth silver thin films deposited with a germanium nucleation layer, Nano Lett. 9 (2008) 178–182.
[28] A.K. Kulkarni, L.C. Chang, Electrical and structural characteristics of chromium thin films deposited on glass and alumina substrates, Thin Solid Films 301 (1997) 17–22.
[29] H. Kaneko, K. Miyake, Effects of transparent electrode resistance on the performance characteristics of electrochemichromic cells, Appl. Phys. Lett. 49 (1986) 112–114.
[30] K.R. Hebert, A relationship among the transport properties of some concentrated aqueous solutions of binary electrolytes, J. Electrochem. Soc. 137 (1990) 3854–3858.
[31] B. Baloukas, J.-M. Lamarre, L. Martinu, Active metameric security devices using an electrochromic material, Appl. Opt. 50 (2010) c41–c49.
[32] B. Baloukas, J.-M. Lamarre, L. Martinu, From passive to active: future optical security devices, Opt. Soc. Am. (2010) PDTuD10.